J Elasticity (2006) 85: 65–83
DOI 10.1007/s10659-006-9071-3

A Quasi-linear Viscoelastic Constitutive Equation for the Brain: Application to Hydrocephalus

C. S. Drapaca · G. Tenti · K. Rohlf · S. Sivaloganathan

Received: 18 November 2005 / Accepted: 20 April 2006 /
Published online: 25 July 2006

Abstract Hydrocephalus is a condition which occurs when an excessive accumulation of cerebrospinal fluid in the brain causes enlargement of the ventricular cavities. Modern treatments of shunt implantation are effective, but have an unacceptably high rate of failure in most reported series. One of the common factors causing shunt failure is the misplacement of the proximal catheter's tip, which can be remedied if the healed configuration of the ventricular space can be predicted. In a recent study we have shown that this is accomplished by a mathematical model which requires as input the knowledge of the speed at which the ventricular walls move inwardly. In this paper we report on a theoretical method of calculating this speed and show that it will become of great practical usefulness as soon as more experimental results become available.

Mathematics Subject Classifications (2000) 74L15/92C10 · 74D10

Key words viscoelasticity · mathematical modeling · hydrocephalus · brain biomechanics · ventricular shunt

C. S. Drapaca
Department of Physiology and Biomedical Engineering, Mayo Clinic,
Rochester, MN 55905, USA
e-mail: drapaca.corina@mayo.edu

G. Tenti · S. Sivaloganathan (✉)
Department of Applied Mathematics, University of Waterloo, Waterloo, ON N2L 3G1, Canada
e-mail: ssivalog@sumathi.uwaterloo.ca

K. Rohlf
Department of Mathematics, Ryerson University, Toronto, ON M5B 2K3, Canada

S. Sivaloganathan
Centre for Mathematical Medicine, Fields Institute, Toronto, ON M5T 3J1, Canada

1. Introduction

Hydrocephalus is a condition in which an excess of cerebrospinal fluid (CSF) accumulates within the brain's ventricular walls with serious consequences if untreated. The modern treatment consists of a CSF shunt implantation in order to transport the excess fluid from the generation site to the resorption site [7]. CSF shunts are an effective but problematic treatment, in that they can fail for a variety of reasons. A recent, prospective, randomized clinical trial has shown a shunt failure rate of about 50% at two years from implantation [6]. Further analysis of the data indicated that the position of the ventricular catheter tip (in the frontal or the occipital horns), and whether the catheter was surrounded by CSF, were risk factors for shunt failure [44]. This suggests that optimal positioning of the catheter's tip, allowing for the inevitable collapse of the ventricles and the growth of the brain and the skull, could reduce the incidence of shunt failure in children.

In a recent study, and with the help of modern image processing techniques, we showed how to predict the final shape of the ventricular space after shunting [9]. However, the method requires as input the velocity of each point of the ventricular wall as it moves inwardly under the decreasing pressure gradient resulting from the shunting process. In order to find this decompression velocity we need to construct a mathematical model for the hydrocephalic brain capable of describing as accurately as possible the dynamics of the unloading process. Following [18], most researchers in this area liken the brain to a microscopic sponge in which the brain tissue by itself may be considered incompressible, while its compliance results from the collapsibility of the cells of the sponge-like parenchyma. Roughly speaking, two approaches have been used in the study of the brain's response to different types of loading. The first- and older-treats the brain as an elastic or viscoelastic material, and uses linear or nonlinear mathematical models in the spirit of engineering practice [10, 16, 21, 33, 35]. The second approach, on the other hand, is more recent and mathematically more sophisticated [20, 30, 39]. Here the models are based on the theory of consolidation [3] in which the brain parenchyma is treated as a porous, linearly elastic solid with Newtonian fluid-filled pores. In both approaches, many of these models have been solved numerically with the help of standard software packages such as ABAQUS [1] and many researchers have extolled the virtues of an entirely numerical simulation of hydrocephalus.

In view of our poor knowledge of the brain's mechanical properties, however, uncritical reliance on numerical simulations appears premature, and it is in this spirit that the following analysis should be taken. Our task here is the calculation of the velocity of each point on the healing ventricular wall after shunt implantation. On physical grounds one would expect this velocity to depend on the location of the point and, in particular, on the curvature of the ventricular wall. However, a recent study of samples from a large data base [6, 43] showed that the dependence on the curvature seems to be small. Hence, in predicting the ventricular boundary velocity, we can reasonably assume that the speed is the same everywhere; this then allows us to make a drastic simplification in the geometry, whereby we replace the actual hydrocephalic brain with a thick-walled hollow cylinder whose ends are tethered so that the strain distribution is planar, and all displacements occur in the radial direction. The thick wall of the cylinder, on the other hand, is assumed to consist of a homogeneous, isotropic, non-linear viscoelastic material, while the hollow is filled with an incompressible Newtonian fluid (representing CSF).

The next important approximation is introduced in the equation of motion, where inertia terms are neglected, thus making the theory a quasi-equilibrium one. This, however, is an excellent approximation in view of the fact that the response of the hydrocephalic brain occurs on a very long time scale, more akin to a diffusive than a wave-like process.

The rest of the paper is structured as follows. In Section 2 we provide the mathematical background and terminology for our adopted constitutive theory, as well as the necessary mathematical details for our parameter estimation procedure. Section 3 gives an account of the theoretical calculation of the velocity of points on the healing surface, and the last two sections contain the results and a critical discussion of them, respectively.

2. Constitutive Equation and Parameter Estimation

The difficulty of developing an accurate constitutive equation for biological tissues is well known and, in the case of the brain, some of the many efforts involved over the past 30 years have been recently reviewed by [21]. The problem of modeling hydrocephalus is particularly challenging, involving as it does quite large strains which tend to make questionable the use of linear models. It is well known, however, that a constitutive equation taking into account the non-linear stress-strain characteristics of living tissue is the quasi-linear viscoelastic (QLV) theory of [15], which has been found to work reasonably well for a large number of tissues [4, 14]. It seems therefore desirable to apply the QLV theory to the brain, as well.

The essence of Fung's approach is the following. Let us consider a cylindrical specimen of viscoelastic material subject to a tensile load, and let λ be the principal stretch ratio in the z direction. As is familiar to anybody who has handled a piece of silicone "silly putty", the response of the system to fast loading (ideally, step loading) is almost purely elastic, while relaxation occurs on a much longer time scale. It is therefore reasonable to assume that the history of the stress response, called *the relaxation function* $K(\lambda, t)$, can be factorized as

$$K(\lambda, t) = G(t)T^{(e)}(\lambda), \quad G(0) = 1, \tag{2.1}$$

where $G(t)$ is a normalized function of time (*the reduced relaxation function*), and $T^{(e)}(\lambda)$ is the elastic response. Next it is assumed that the stress response to infinitesimal changes in stretch can be evaluated with the Boltzmann superposition principle, which lead up to the following Stieltjes integral

$$T^{(ve)}(t) = \int_{-\infty}^{t} G(t-\tau)\frac{\partial T^{(e)}(\lambda(\tau))}{\partial \lambda} d\lambda(\tau), \tag{2.2}$$

or, since $G(t)$ is assumed to be continuously differentiable, to

$$T^{(ve)}(t) = T^{(e)}(\lambda(t)) + \int_{-\infty}^{t} T^{(e)}(\lambda(t-\tau))G'(\tau)d\tau. \tag{2.3}$$

Thus the tensile stress of the viscoelastic material $T^{(ve)}$ at any time t is equal to the instantaneous stress response $T^{(e)}$ decreased by an amount depending on past history (since $G'(t) < 0$).

The next step in the derivation of the constitutive equation is the development of appropriate models for the elastic response $T^{(e)}$ and for the relaxation function G.

Among the many possibilities, the Mooney–Rivlin [27] approach recommends itself for its simplicity and success in modeling $T^{(e)}$ for incompressible, isotropic, rubber-like materials, in which case it can be shown that a strain energy function Σ exists [2] and has the form

$$\Sigma = C_{10}(I_1 - 3) + C_{01}(I_2 - 3), \tag{2.4}$$

where C_{10}, C_{01} are the Mooney–Rivlin coefficients and I_1, I_2 are the principal invariants of the left Cauchy–Green stretch tensor. It follows from this (see [8], for the mathematical details) that the stress tensor takes the form

$$T^{(e)} = 2\left(\lambda^2 - \frac{1}{\lambda}\right)\left(C_{10} + \frac{C_{01}}{\lambda}\right). \tag{2.5}$$

As for the reduced relaxation function, we adopt the popular box-shaped spectrum [4, 5, 14, 31, 36, 37] which leads to the formula

$$G(t) = \frac{1 + c\left[Ei\left(\frac{t}{\tau_2}\right) - Ei\left(\frac{t}{\tau_1}\right)\right]}{1 + c\ln\left(\frac{\tau_2}{\tau_1}\right)}, \tag{2.6}$$

where $Ei(x) = \int_x^\infty \frac{e^{-x}}{x}dx$ is the exponential integral function, the parameter τ_1 governs fast relaxation processes (the larger τ_1, the faster the initial relaxation), τ_2 governs the slow processes (the larger τ_2, the longer relaxation takes), and c determines the degree to which viscous effects are present ($c = 0$ when only the elastic response is present). It is then straightforward to derive from (2.3), (2.5) and (2.6) the final form of the QLV stress tensor as

$$T^{(ve)}(t) = \int_{-\infty}^{t} G(t-\tau)H(\lambda(\tau))\lambda'(\tau)d\tau, \tag{2.7}$$

where

$$H(\lambda(\tau)) = C_{10}\left[4\lambda(\tau) + \frac{2}{\lambda^2}\right] + C_{01}\left[2 + \frac{4}{\lambda^3(\tau)}\right]. \tag{2.8}$$

As is clear from these expressions, our QLV constitutive equation involves five unknown parameters – c, τ_1, τ_2, C_{10} and C_{01} – Which must be determined from experiment; and this is a delicate task for the following reasons.

Normally, one would extract the material parameters by fitting the material functions directly to the data. To be consistent with the assumptions of the QLV theory, the material functions should be obtained by subjecting the test sample to an instantaneous change to a value λ_0 of the stretch ratio at $t = 0$, followed by a holding of the stretch λ_0 for $t > 0$. Unfortunately, such experimental conditions are not realizable and one usually must settle for a determination of the elastic response from a "fast" stretch ramp $[0, \lambda_0]$ in time t_0.

No fewer problems will be encountered by attempting to match $G(t)$ directly to relaxation data. In particular, the assumption that material relaxation ends when the experiment is stopped is unwarranted [5, 29], for it is understood that the loading rate affects the stress relaxation [22, 38] and that stress relaxation can continue well beyond the time allowed in typical experiments [14].

Table 1 Material parameters for different strain rate values

Strain rate v [ips]	C_{10} [psi]	C_{01} [psi]	c	τ_1 [s]	τ_2 [s]
0.2	0.23	0.09	0.36	0.5	80
2	0.14	0.67	0.33	0.5	80
10	0.27	0.73	0.32	0.5	80

A clever method to obviate these difficulties has been recently developed by [4] and used in their application of QLV theory to the internal shearing of porcine aortic valve leaflets. In their words,

> We fit the loading and relaxation data separately and relate these to the equivalent instantaneous loading experiment by imposing the constitutive equation at the start and end of relaxation. The reduced relaxation function is obtained through normalizing by the infinite-strain-rate stress, as required by the QLV theory. This follows a fit of dimensional relaxation data by a relaxation function. The elastic response is obtained from a scale-up of the measured stress in the loading part of the experiment. ([4], p.387).

The effect of this procedure is that the values of the extracted parameters are those for which the constitutive Equation (2.7) predicts the fast strain-rate experiments, rather than those for which the material functions directly match the data, with the consequence that the latter are more realistic estimates of the "true" material functions. This procedure for the extraction of the material parameters, adjusted for our case, is reviewed in Appendix A, along with a discussion of the experiments used for the fitting procedure. The values of the extracted parameters are listed in Table 1 of the Results section.

3. Equation of Motion and Derivation of the Speed of the Healing Surface

The QLV constitutive Equation (2.7), derived by the method summarized in the previous section, allows us to write down the equation of motion and the appropriate boundary conditions, which can then be solved for the displacement vector and hence the velocity of the healing surface. This task sounds straightforward in principle, but it is nothing of the sort in practice. In particular, we shall pay attention to the appropriate form of the stress tensor at various stages of the calculation, as there is some confusion in the literature.

As stated in the Introduction, our previous work [9] has shown that the healing velocity has a relatively small dependence on the curvature of the ventricular walls, which means that all points of these surfaces move with approximately the same speed in response to the reduced ventricular pressure caused by shunt drainage. Consequently, we may model the brain as a thick-walled, viscoelastic, hollow cylinder whose outer elastic casing represents the skull. The outer skull is modelled as an elastic casing to permit the inward motion of the outer skull on decompression drainage – As commonly occurs in pediatric hydrocephalic patients. It is important to keep in mind, however, that *this simplified geometry is only used for the purpose of calculating the healing speed*, which is then used for the study of the actual

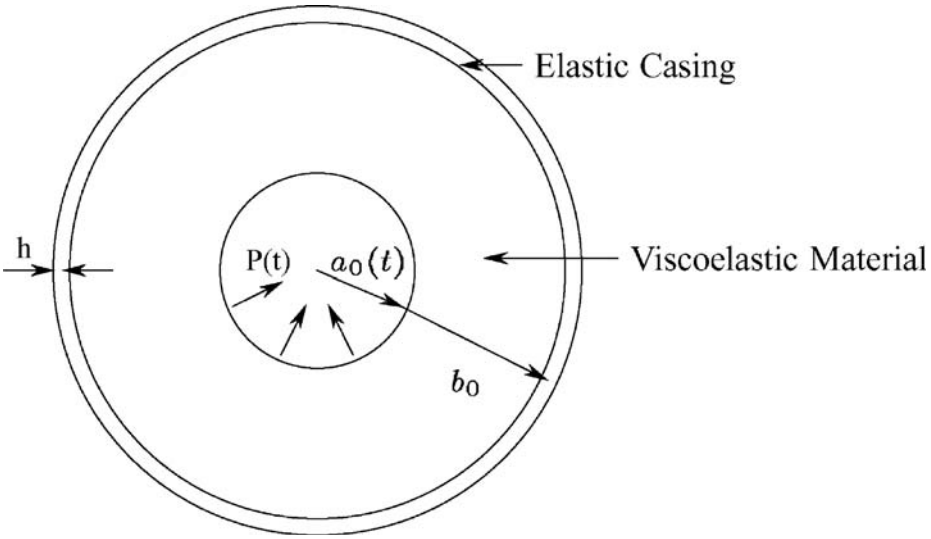

Figure 1 Geometry of a quasi-linear viscoelastic cylinder with healing inner surface and reinforced by an elastic casing in the reference configuration.

hydrocephalic brain. We also assume that the material is homogeneous, isotropic, and incompressible, and that the motion of the healing surface is radial.

Consider now a cross-section of the cylinder as in Figure 1. Thanks to the incompressibility condition we have

$$\pi \left[r^2 - a^2(t)\right] = \pi \left[R^2 - a_0^2(t)\right], \tag{3.1}$$

where $a_0(t)$ and b_0 are the inner and outer radii of the reference cylinder, $a(t)$ and b are the inner and outer radii of the current cylinder, and (R, Θ, Z) and (r, θ, z) are the standard cylindrical coordinates of a material particle before and after deformation, respectively. Since the inner cylinder is not only de-pressurized but also is shrinking (due to the natural growth of the brain tissue), its radius is a function of time $a_0(t)$ which is assumed to be known (i.e. by giving $a_0(t)$ we prescribe the law of normal, natural growth phenomena that occur in *any* – hydrocephalic or normal – brain tissue). It is convenient to introduce the quantity

$$A(t) = a^2(t) - a_0^2(t), \tag{3.2}$$

which has obviously the dimensions of area, so that Equation (3.1) can be rewritten as $r^2 = R^2 + A(t)$. It is then clear that the deformation law in response to the internally decreasing pressure $P(t)$ is given by

$$\begin{cases} r = \sqrt{R^2 + A(t)}, \\ \theta = \Theta, \\ z = Z. \end{cases}$$

The deformation gradient is therefore

$$\mathbf{F} = \begin{pmatrix} \dfrac{R}{\sqrt{R^2 + A(t)}} & 0 & 0 \\ 0 & 1 & 0 \\ 0 & 0 & 1 \end{pmatrix}, \tag{3.3}$$

and the only two nonvanishing physical components of the strain tensor are:

$$E_{RR} = -\frac{A(t)}{2(R^2 + A(t))}, \quad E_{\Theta\Theta} = \frac{A(t)}{2R^2}. \tag{3.4}$$

Thus, the kinematic description of the motion is known as soon as $A(t)$ is known. The dynamics of the motion, on the other hand, requires the solution of the Cauchy equation

$$\rho \ddot{\vec{u}}^{(ve)} = \mathrm{div}\mathbf{T}^{(ve)} + \rho \vec{f}, \tag{3.5}$$

where $\vec{u}^{(ve)}$ is the displacement vector, $\vec{f}$ the resultant of the external forces, $\mathbf{T}^{(ve)}$ is the Cauchy stress tensor, and all quantities are expressed in the current (deformed) configuration. Because of our interest in hydrocephalus, which is notoriously a very slow process, we may drop the inertia terms (which characterize wave motions) and neglect the external forces as well, in order to simplify the equation of motion as much as possible. All that remains of Equation (3.5) is then $\mathrm{div}\mathbf{T}^{(ve)} = \vec{0}$, which has the form of a static problem. Unfortunately, the boundary conditions complicate matters considerably; for they must express the matching of the stresses at the interface separating the liquid from the viscoelastic medium, and in the current configuration such a boundary is not known.

We circumvent this problem by switching to the reference configuration in which the geometry of the ventricles is known *a priori*. Even though the reference configuration is usually chosen to be the undeformed one, it is not essential that it be so ([2], p.1702); in our case the reference configuration can be defined to be any intermediate configuration determined by CT scans. Then our boundary value problem becomes:

$$\mathrm{Div}\left(\mathbf{F}\mathbf{\Pi}^{(ve)}\right) = \vec{0}, \tag{3.6}$$

$$\Pi_{RR}^{(ve)}(a_0(t), t) = P(t), \tag{3.7}$$

$$\Pi_{RR}^{(ve)}(b_0, t) = B\, E_{\Theta\Theta}(b_0, t), \tag{3.8}$$

where the deformation gradient $\mathbf{F}$ is given by Equation (3.3), the strain tensor $\mathbf{E}$ is given by Equation (3.4), $\mathbf{\Pi}^{(ve)}$ is the second Piola–Kirchhoff stress tensor, and $\dfrac{a_0(t)}{a(t)} P(t)$ represents the contact force in the current configuration per unit area of the inner surface in the reference configuration. The constant B is given by [35]:

$$\frac{1}{B} = \left[1 + \frac{b_0}{h}(1 - \nu)\right] \frac{1 + \nu}{E}, \tag{3.9}$$

where h, ν and E are the thickness, Poisson ratio and, respectively, the Young modulus of the elastic casing. Everything in Equations (3.6)–(3.8) is referred to the reference configuration in which the cylindrical coordinates are R, Θ, Z. The

coordinate switch must be applied, of course, to the QLV constitutive Equation (2.2) as well, and it is a simple matter to show [8] that in the reference configuration it becomes

$$\mathbf{\Pi}^{(ve)}(R,\,t)\,=\,\int_0^t G(t-\tau)\frac{d}{d\tau}\mathbf{\Pi}^{(e)}(R,\,\tau)d\tau, \tag{3.10}$$

where the relaxation function G is given by Equation (2.6) and $\mathbf{\Pi}^{(e)} = \mathbf{F}^{-1}\dfrac{\partial\,\Sigma(\mathbf{F})}{\partial\mathbf{F}}$ is the second Piola–Kirchhoff tensor in the corresponding elastic solid with $\Sigma(\mathbf{F})$ given by Equation (2.4). A straightforward calculation (Drapaca [8], Ch.5) produces the explicit forms of the only two nonvanishing physical components of the second Piola–Kirchhoff tensor as

$$\Pi^{(e)}_{RR}\,=\,-\frac{p^{(e)}\left[R^2+A\,(t)\right]}{R^2}+2C_{10}-2C_{01}\frac{\left[R^2+A\,(t)\right]^2}{R^4}, \tag{3.11}$$

$$\Pi^{(e)}_{\Theta\Theta}\,=\,-\frac{p^{(e)}R^2}{\left[R^2+A\,(t)\right]}+2C_{10}-2C_{01}\frac{R^4}{\left[R^2+A\,(t)\right]^2}, \tag{3.12}$$

where $p^{(e)}$ is the indeterminate scalar arising from the constraint of incompressibility [45].

It is well known that one of the powerful techniques for solving boundary value problems in linear viscoelasticity is the use of the correspondence principle (also known as the *elastic-viscoelastic analogy*). Generally, viscoelastic stress analysis problems are more involved than elasticity problems due to the inclusion of the time variable in the regulating equations. However, in many problems where the types of boundary conditions and the temperature remain constant in time, the time variable can be removed by using the Laplace transform. The problem is then converted into an equivalent elastic problem; when the latter has been solved the inverse Laplace transform of the result will produce the full solution of the original viscoelastic problem [13, 17].

As it stands, the classical elastic-viscoelastic analogy does not apply to our case. However, the solution to our QLVE boundary problem can be easily constructed from the solution of an elastic problem as follows. Let $D(t)$ be the creep function given by

$$\int_0^t G(t-\tau)\frac{dD(\tau)}{d\tau}d\tau\,=\,H(t), \tag{3.13}$$

where $G(t)$ is the given relaxation function and H is the unit step function. If we take the convolution of Equations (3.6)–(3.8) with the time derivative of the creep function $D(t)$ and make use of relation (3.13), the properties of the convolution operation and the definition of the Dirac distribution (since the derivative of H is the Dirac function), we obtain the following hyperelastic problem

$$\text{Div}\,\left(\mathbf{F}\mathbf{\Pi}^{(e)}\right)=\vec{0}, \tag{3.14}$$

$$\Pi^{(e)}_{RR}\,(a_0(t),\,t)=\int_0^t D(t-\tau)\frac{d\,P(\tau)}{d\tau}d\tau, \tag{3.15}$$

$$\Pi^{(e)}_{RR}\,(b_0,\,t)=B\int_0^t D(t-\tau)\frac{d\,E_{\Theta\Theta}(b_0,\,\tau)}{d\tau}d\tau, \tag{3.16}$$

which corresponds to the original viscoelastic problem given by Equations (3.6)–(3.8).

By substituting (3.11) and (3.12) into Equation (3.14), one easily isolates the term $\partial p^{(e)}/\partial R$ which can then be simply integrated to obtain $p^{(e)}$. This is next substituted into (3.11) with the result

$$\Pi^{(e)}_{RR}(R,t) = -\frac{R^2 + A(t)}{R^2} f(t) + 2C_{10} - (C_{01} - C_{10})\frac{A(t)}{R^2} - \\ - (C_{10} + C_{01})\frac{R^2 + A(t)}{R^2}\ln\left(\frac{R^2 + A(t)}{R^2}\right) - 2C_{01}\frac{R^2 + A(t)}{R^2}, \quad (3.17)$$

where $f(t)$ is an arbitrary function of time arising from the process of integration with respect to R of the equation for $\partial p^{(e)}/\partial R$. Since the Mooney–Rivlin coefficients C_{01} and C_{10} will be determined in the next section, the only unknowns are the two functions of time $A(t)$ and $f(t)$, and these are determined by the boundary conditions (3.15) and (3.16). The procedure is quite straightforward. Recalling that $E_{\Theta\Theta}(R, t) = \frac{A(t)}{2R^2}$, substitution of this and of (3.17) into (3.15) and (3.16) produces a system of two equations in two unknowns, and elimination of $f(t)$ gives us the following integro-differential equation for $A(t)$:

$$(C_{01} + C_{10})\left[\ln\left(\frac{1 + \frac{A(t)}{b_0^2}}{1 + \frac{A(t)}{a_0^2(t)}}\right) + \frac{1}{1 + \frac{A(t)}{a_0^2(t)}} - \frac{1}{1 + \frac{A(t)}{b_0^2}}\right] \\ + \frac{B}{2\left(b_0^2 + A(t)\right)}\int_0^t D(t-\tau)\frac{dA(\tau)}{d\tau}\,d\tau \\ - \frac{1}{1 + \frac{A(t)}{a_0^2(t)}}\int_0^t D(t-\tau)\frac{dP(\tau)}{d\tau}\,d\tau = 0. \quad (3.18)$$

The presence of the constant B in Equation (3.18) accounts for the effect of the elastic casing on the solution $A(t)$.

Once the function $A(t)$ is known, the radial displacement in the viscoelastic cylinder can be found from

$$U^{(ve)}(R, t) = \sqrt{R^2 + A(t)} - R \quad (3.19)$$

and thus the healing velocity can be immediately calculated. The numerical solution of Equation (3.18) is discussed in Section 4.

4. Results

The choice of the method of [4] for the determination of our parameters was explained in Section 2, and the method itself is reviewed in Appendix A. In this section we report on the results of this fitting procedure to the experiments of [12] and [16]. The former gives loading data from the sample compression at the constant rates of 0.02, 0.2, 2 and 10 ips (inches per second – See Appendix A, last paragraph);

with L denoting the initial length of the cylindrical sample, and v the compression rate, the stretch ratio at any time instant t was given by $\lambda = 1 + (v/L)t$. The latter experiment was performed by holding the stretch ratio at the constant value λ_0 such that the initial relaxation modulus is $T_0 = 0.95$ psi (1 psi $= 6.89 \times 10^3$ Pa); only the first 80 s of the relaxation process were recorded, and the value of the relaxation stress at time $t_1 = 80$s was $T_1 = 0.32$ psi.

These experimental results were published in the same year but in two separate papers. However, in order to find our parameters we need to assume that the *same* brain tissue specimen was used in a fast-loading test followed by relaxation. Consequently, we chose to mimic a single *load and hold* test by the following *cut and paste* procedure:

1 From the fast loading experiments we find the time t_0, and hence the stretch ratio $\lambda_0 = 1 + (v/L)t_0$ from which $T^{(ve)}(t_0) = \sigma^E(\lambda_0) = T_0 = 0.95$ psi.
2 We assume $\lambda = \lambda_0 =$ constant and use the relaxation data from [16] on the same sample as in the previous step. Taking into account that the last recorded relaxation datum is at time $t = 80$s where the relaxation stress is 0.32 psi, we choose $t_1 = 80$ s and $T^{(ve)} = T_1 = 0.32$ psi.

The above steps are summarized graphically in Figure 2. The fitting algorithm outlined in Appendix A is then used and parameter values so obtained are listed in Table 1. We note here that the loading rate of 0.02 ips was deemed too slow to be compatible with the QLV theory, and was therefore not used. Furthermore, no attempt has been made to supply an estimate of the error because of too many uncertainties in the data which we had read off the published figures. Hence, we simply rounded off the results of the calculations to two decimal places, and elaborate on their status in the next section.

Having determined the values of the parameters, and having therefore obtained the QLV constitutive Equations (2.7)–(2.8), we are now ready to move to seeking the solution of the dynamical equations; and, as explained in Section 3 and in Appendix B, this means finding a solution to Equation (3.18) which can only be done numerically.

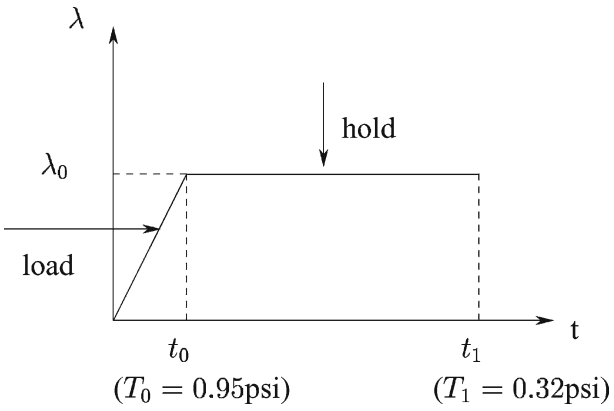

Figure 2 Loading and relaxation tests for the human brain tissue: The loading experiment is *cut* when $T^{(ve)}(t_0) = 0.95$ psi and is *pasted* to the relaxation experiment which is recorded till $T^{(ve)}(t_1) = 0.32$ psi.

We start out by prescribing the values of c, τ_1 and τ_2. Using the fastest compression rate listed in Table 1, we set $c = 0.32$, $\tau_1 = 0.5$ s and $\tau_2 = 80$ s, and obtain from Equation (2.6) the relaxation function:

$$G(t) = 0.38 + 0.12\left[Ei\left(\frac{t}{80}\right) - Ei\left(\frac{t}{0.5}\right)\right]. \tag{4.1}$$

Next we expand the exponential integrals in a power series about $t = 0$, substitute into Equation (3.13) and take the Laplace transform of the result; this gives the Laplace transform of $D(t)$, from which we obtain the creep function upon taking the inverse Laplace transform. The result is:

$$D(t) = 0.25e^{0.12t}\sin(0.47t) + 1.01e^{0.12t}\cos(0.47t) \tag{4.2}$$

and is plotted in Figure 3 over the normalized, dimensionless, time interval $[0,\ 1]$.

We notice that $D(t)$ varies from 1.01 to 1.14 over the normalized time interval $[0,\ 1]$, which is a variation of about 10%; thus, given the uncertainty about the data,

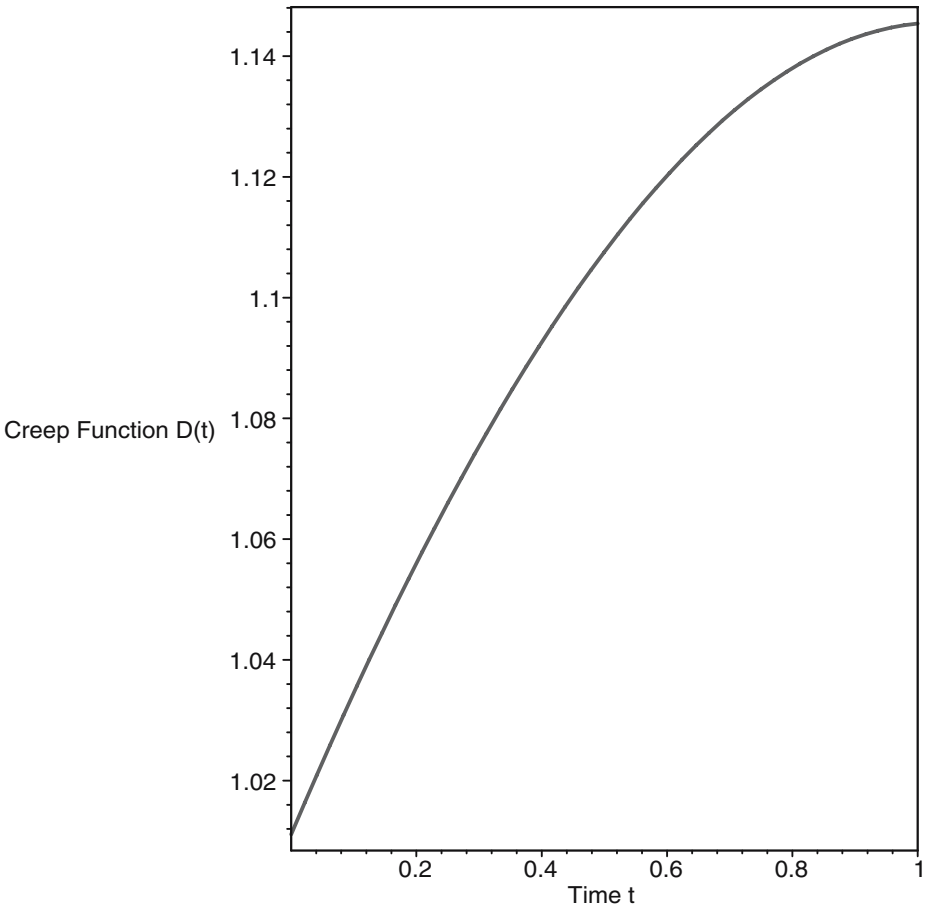

Figure 3 Creep function *versus* time.

we simplify the creep function to the constant $D(t) = 1$, which says that theviscoelastic stress and the corresponding nonlinear elastic stress are approximately the same. With this approximation, the equation for $A(t)$ given by (3.18) becomes:

$$(C_{01}+C_{10})\left[\ln\left(\frac{1+\dfrac{A(t)}{b_0^2}}{1+\dfrac{A(t)}{a_0^2(t)}}\right)+\frac{1}{1+\dfrac{A(t)}{a_0^2(t)}}-\frac{1}{1+\dfrac{A(t)}{b_0^2}}\right]$$
$$+\frac{B}{2\left(b_0^2+A(t)\right)}A(t)-\frac{1}{1+\dfrac{A(t)}{a_0^2(t)}}(P(t)-P(0))=0. \tag{4.3}$$

Next we need to select values for C_{01}, C_{10}, $a_0(t)$, b_0, and B. The first two are already displayed in Table 1, given by 0.73 and 0.27 psi, respectively. The next three are more difficult to determine, as we have no experimental values to rely upon, and all we know from the formulation of our problem is that $a_0(t)$ and $P(t)$ must be decreasing functions of time. We note, however, that the viscoelastic cylinder with a fixed elastic casing has been well studied [19, 28, 35, 40–42] and for the purpose of our simulation we introduce the following characteristic quantities: A characteristic length as $l_c = a_0(0)$ [length units], a characteristic time $t_c = 24$ [months] [32], and a characteristic pressure $P_c = C_{01}+C_{10} = 1$ [psi]. The dimensionless quantities of our problem are:

$$\tau = \frac{t}{t_c},\ \tilde{b}_0 = \frac{b_0}{l_c} = 2,\ \tilde{h} = \frac{h}{l_c} = 0.01,\ \nu = \frac{1}{2},\ \tilde{E} = \frac{E}{P_c},$$
$$\tilde{A}(\tau) = \frac{A(\tau)}{l_c^2},\ \tilde{a}_0(\tau) = \frac{a_0(\tau)}{l_c} = \frac{1}{\sqrt{1+\left(1-\dfrac{a_0(0)^2}{b_0^2}\right)\tau}},$$
$$\tilde{P}(0) = \frac{P(0)}{P_c} = 0.01,\ \tilde{P}(\tau) = \frac{P(\tau)}{P_c} = \tilde{P}(0)\left[2+\frac{-1+e^{-\tau}}{1-\mathrm{e}^{-1}}\right], \tag{4.4}$$

and the constant B given by (3.9) becomes in this case:

$$\frac{1}{B} \approx \frac{1}{0.006E}. \tag{4.5}$$

We assumed that the pressure decreases from twice the normal CSF pressure to the normal CSF pressure which is 0.01 psi. Finally, we substitute the above quantities into Equation (4.3) and use *Maple VI's* function *fsolve* [23] to get the numerical values of $\tilde{A}(\tau)$ (and hence the values of $A(t)$). The parameter B is determined by the Young modulus E of the elastic casing, which in our application represents the presence of the skull (at least for hydrocephalus in the adult). Unfortunately, the value of E is not well known, and so, for the moment, B has to be considered a free parameter. Nevertheless, we have attempted to determine at least a bound for B in the following manner.

The assessment of changes in ventricular volume on serial computed tomography (CT) and magnetic resonance imaging (MRI) studies is extremely important for the evolution and treatment of patients with symptoms of recurring hydrocephalus or possible shunt malfunction. For this reason neurosurgeons have developed over the years practical and objective methods of making such assessments. One of

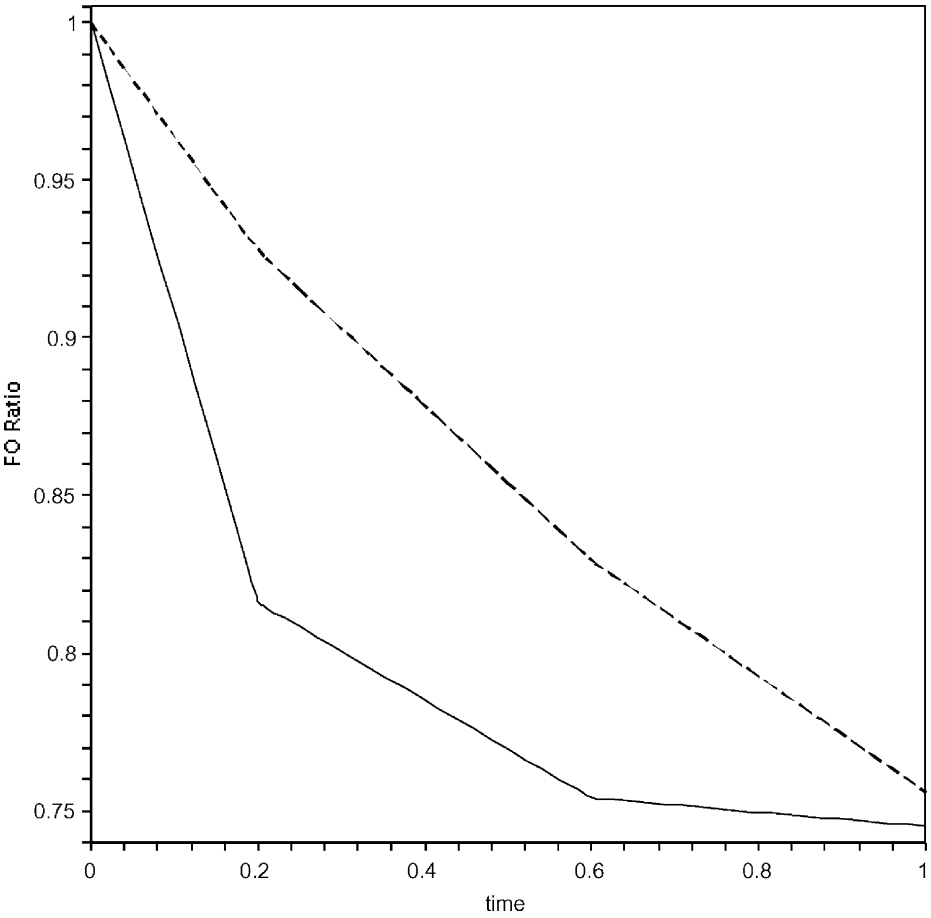

Figure 4 FO ratio estimates of the sigma shunt (*solid line*) and of our model (*dashed line*).

these, known as the frontal-occipital (FO) ratio, estimates the ventricular size by consideration of the arithmetic average of the distance between the frontal and the occipital horns normalized to the skull's diameter [32], and a typical result obtained by this method is shown with a solid line in Figure 4. The straight segments shown as solid lines in Figure 4 are simple linear interpolations between the experimental points for the sigma shunt [43], and their slopes can be taken as rough experimental estimates of the ventricular healing speeds (solid line in Figure 5). Since the FO ratio corresponding to our model is $\tilde{a}(\tau)/\tilde{b}$, the ventricular healing speed predicted by our model is

$$\tilde{v}(\tau) = \frac{d}{d\tau}\left(\frac{\tilde{a}(\tau)}{\tilde{b}}\right). \tag{4.6}$$

The result of the comparison between the theoretical and experimental FO ratios and speeds are shown in Figures 4 and 5, respectively. A value of $E \approx 0.16 \times 10^5$ psi (or $E \approx 11$ MPa) gives the best approximation to the data. Since the skull is

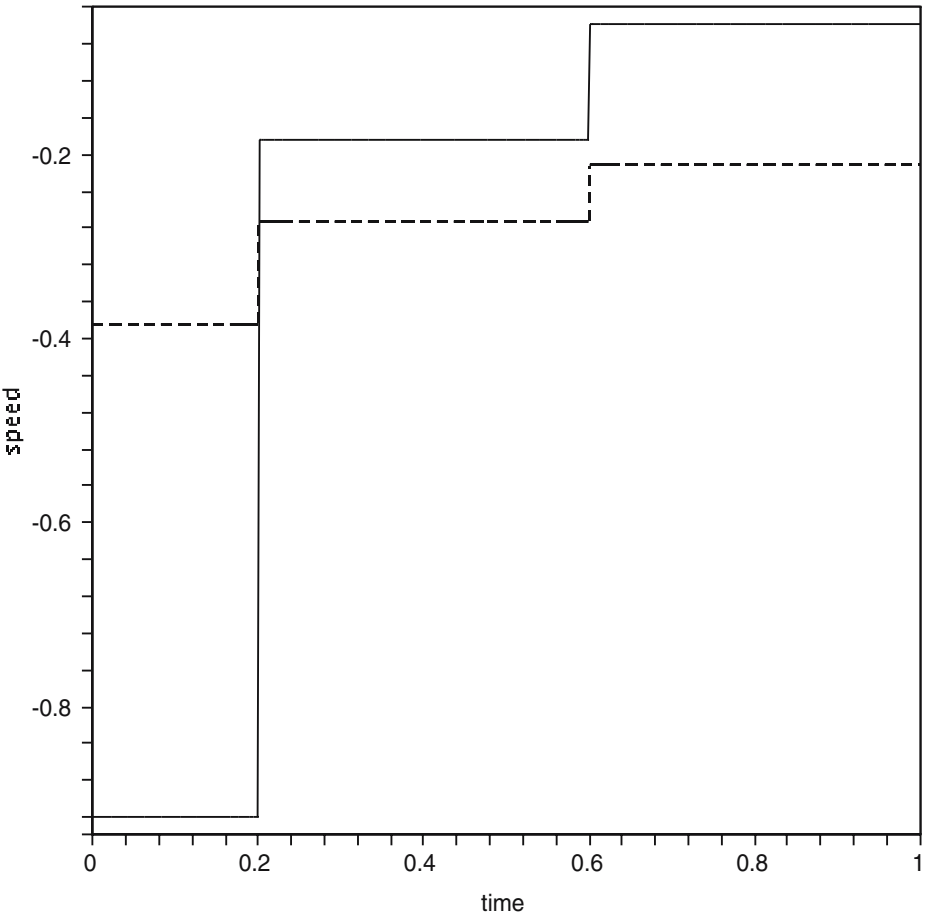

Figure 5 Speed estimates of the sigma shunt (*solid line*) and of our model (*dashed line*).

certainly much less stiff than, say, steel ($E \approx 200$ GPa) this result is not unreasonable; nevertheless, we will argue in the next section that it is subject to serious doubts.

5. Discussion and Conclusions

In this work we have presented a method for deriving the constitutive equation for brain matter, and we have shown how it can be used in shunted hydrocephalus to predict the speed of points on the ventricular walls resulting from the induced decompression.

The theory takes into account several important considerations. First, like all biological tissues, the brain tissue is not elastic, as the strain history affects the stress distribution. In particular, there is considerable difference in stress response to loading and unloading [14], and nonlinear effects must be considered due to the large strains involved in hydrocephalus. Consequently, we have developed a constitutive

equation (Equations (2.2) or (2.3)) based on the well-known QLV theory [15], in which the elastic response was modeled with the classical Money–Rivlin approach (Equations (2.4) and (2.5)) and the reduced relaxation function with the popular box-shaped spectrum (Equation (2.6)). The resulting five unknown parameters were determined from the data of [12] and [16] by the fitting protocol developed by [4]. In addition, we assumed that our QLV model of the brain tissue behaves alike in compression and in decompression.

The same set of data was used in the past to determine the Mooney–Rivlin parameters C_{10} and C_{01} [24] on the assumption that brain tissue can be considered as an incompressible viscoelastic material under quasi-static loading conditions. This assumption was later questioned by [25] who fairly pointed out that the high compression rates used by Estes and McElhaney can hardly be considered suitable for the determination of static or quasi-static properties of the brain tissue. And in the intervening years, Miller and collaborators have produced several sets of data taken at much lower strain rates (as deemed appropriate for surgical procedures), including data from brain tissue in tension [26].

Unfortunately, these data are not useful to us. The elastic response $T^{(e)}$ in the QLV theory is the stress generated instantaneously in the tissue when a step function of stretching λ is imposed on the specimen ([14], p.279). Thus, as already pointed out, we need loading data at very large strain rates, and, so far as we know, the old measurements performed by the McElhaney group are the only suitable ones for us, albeit far from ideal for the following reason.

The clever method of parameter fitting developed by [4] – and reviewed in Appendix A – bypasses the problem of having to decide whether relaxation stops when the experiment stops, or else of having to wait for an inordinately long amount of time. However, it requires the procedure to be based on a *load-and-hold* type of experiment, which does not appear to have been the case in the data of McElhaney and collaborators. Hence, we have used the *cut-and-paste* procedure explained in Section 4 in order to illustrate our procedure for the extraction of the material parameters values listed in Table 1. This means, of course, that these values must be taken with a grain of salt, and we are looking forward to new and appropriate data which would permit an accurate determination of these very important parameters.

A second crucial feature of our theory is its ability to handle the complicated boundary value problem arising from the dynamics (Equations (3.6)–(3.8)). As is frequently the case with this type of problem, the difficulty lies in the form of the boundary conditions, which embody much of the physics and are to be enforced on time-dependent surfaces. If, despite the time dependence, the boundary surfaces do not change form, then the powerful correspondence principle can be used to solve the problem [13, 17]. In our case, however, the principle does not apply, for the matching of the radial stress and the ventricular pressure must be maintained on the healing surface whose shape changes in time, as Equation (3.7) shows. Fortunately, by using the relation between the creep and the relaxation functions (3.13) and properties of the convolution operation, we were able to solve our viscoelastic problem (3.6)–(3.8) by transforming it into a boundary value problem for the corresponding hyper-elastic body (3.14)–(3.16).

A third aspect of this work is rather technical, but all the same quite important. As is well known, the deformation of an elastic or viscoelastic body can be described with respect to a reference configuration or with respect to the current (deformed) configuration. The former description is generically known as the Lagrangian

representation while the latter is called Eulerian; and each one has its own expressions for the stress and the strain tensors. When the mathematical theory is linear, there is no difference in the form of the stress and strain tensors in the two representations; but when we deal with large deformations we must include nonlinear terms, and then the stress and the strain tensors are quite different, and one must use one representation or the other in a mathematically consistent fashion. It is unfortunate that there is a certain amount of confusion in the literature about this point. For example, in some interesting work on the development of approximate constitutive equations for nonlinear viscoelastic materials done a few decades ago [19] there is confusion between the Cauchy and Piola stress tensors, and the confusion persists in subsequent works [40–42].

We have been careful to use the appropriate tensor representation at each stage of the calculation, and to make sure that the reader appreciates that different names are used in the biomechanics literature for the same mathematical object. Thus, for example, the Lagrangian stress tensor, the first Piola–Kirchhoff tensor, and the 'engineering stress tensor' refer to the same object, namely the expression of the stress components in the reference configuration. Furthermore, the components of a tensor do not necessarily have the same physical dimensions, and we can illustrate this by showing the form of the Green strain tensor for our viscoelastic cylinder [9]; that is, the non-zero components of the strain tensor **E** in the reference configuration are given by

$$E_{RR} = -\frac{A(t)}{2(R^2 + A(t))}, \quad E_{\Theta\Theta} = \frac{A(t)}{2}, \tag{5.1}$$

where it is obvious that the physical dimensions are different (pure number (or scalar) *versus* area). Instead, we have used the so-called *physical components* of the strain [11], where the second relation in Equation (5.1) is replaced by $E_{\Theta\Theta} = \dfrac{A(t)}{2R^2}$, which is also a scalar.

In conclusion, the theory presented here represents, in our view, a substantial step forward in the area of Brain Biomechanics. Because of the manner in which the constitutive equation was derived, the theory is general enough to cover high-frequency (trauma) as well as low-frequency (hydrocephalus) phenomena. Furthermore, the method of parameter extraction is robust, in that it does not depend crucially on the experimental way in which relaxation data are collected. The weakness only resides in the lack of appropriate data, but we are hopeful that this work will stimulate the experimental researchers in this area to soon remedy this situation.

Acknowledgments This work was supported in part by the Natural Sciences and Engineering Research Council of Canada (NSERC) through a Collaborative Health Research Grant. We would like to thank the anonymous referees for their very helpful comments and suggestions.

Appendix A: Parameter Estimation

Following Carew et al. [4] we rewrite the elastic response $T^{(e)}$ given by Equation (2.5) in a form more convenient to the fitting protocol, namely

$$T^{(e)} = \beta \frac{\sigma^E(\lambda)}{\sigma^E(\lambda_0)}, \tag{A.1}$$

where

$$\sigma^E(\lambda) = \bar{C}_{10}\left(\lambda^2 - \frac{1}{\lambda}\right) + \bar{C}_{01}\left(\lambda - \frac{1}{\lambda^2}\right), \tag{A.2}$$

and

$$\bar{C}_{10} = 2C_{10}\sigma^E(\lambda_0)/\beta,\ \bar{C}_{01} = 2C_{01}\sigma^E(\lambda_0)/\beta. \tag{A.3}$$

The parameter $\beta = T^{(e)}(\lambda_0)$ is the instantaneous elastic stress due to the step-stretch ratio λ_0, and the function $\sigma^E(\lambda)$ can be fitted to the measured stress-stretch ratio data, which are then scaled up by an amount equal to the ratio of instantaneous measured stress at stretch λ_0.

Similarly, the reduced relaxation function $G(t)$ given by Equation (2.6) is rewritten as

$$G(t) = \sigma^r(t,\ \lambda_0)/\sigma^r(0,\ \lambda_0), \tag{A.4}$$

where

$$\sigma^r(t,\ \lambda) = \alpha\left\{1 + c\left[Ei\left(\frac{t}{\tau_2}\right) - Ei\left(\frac{t}{\tau_1}\right)\right]\right\} \tag{A.5}$$

and the parameter α is the stress remaining in the material after relaxation. Furthermore, by imposing continuity of the elastic response and the relaxation function at $t = 0,\ \lambda = \lambda_0$, we obtain the consistency equation

$$T^{(ve)} = \sigma^r(0,\ \lambda_0) = \alpha\{1 + c\ln(\tau_2/\tau_1)\} = T^{(e)}(\lambda_0) = \beta, \tag{A.6}$$

which follows by substitution of Equations (A.1) and (A.4) into Equation (2.3) of the text.

The algorithm for finding the material parameters is then the following:

Step 1: Fit the fast strain-rate loading data to $\sigma^E(\lambda)$ in order to obtain $\bar{C}_{10}$ and $\bar{C}_{01}$. Only β is then required for the complete specification of the elastic response.

Step 2: Fit the relaxation data to Equation (A.5) and get $\alpha^{(1)}$, $(\alpha c)^{(1)}$, $\tau_1^{(1)}$, and $\tau_2^{(1)}$, where the superscripts represent the number of updates to those parameters. The corresponding $\beta^{(1)}$ is obtained from the consistency condition (A.6).

Step 3: Since in Step 2 the fitting algorithm is more sensitive to the initial values of τ_2 and (αc), we fix α and τ_1 to $\alpha^{(1)}$ and $\tau_1^{(1)}$, and update β, (αc), and τ_2. As explained in the main text after Equation (2.8), we impose the constitutive Equation (2.3) at time t_0 and obtain the relation

$$T_0 = \beta + (\alpha c) I_0(t_0,\ \tau_1,\ \tau_2)/T_0, \tag{A.7}$$

where

$$I_0 = \int_0^{t_0} \sigma^E(\lambda(t_0 - s))(\exp(-s/\tau_1) - \exp(-s/\tau_2))/s\,ds \tag{A.8}$$

and $\lambda(t) = 1 + \dfrac{v}{L}t$, with v the loading speed (see below).

Next, the constitutive equation is imposed at t_1, leading to

$$T_1 = \beta + (\alpha c)\left[I_{01}(t_0,\ t_1,\ \tau_1,\ \tau_2) + I_1(t_0,\ t_1,\ \tau_1,\ \tau_2)/T_0\right], \tag{A.9}$$

where

$$I_{01} = \int_0^{t_1-t_0} (\exp(-s/\tau_1) - \exp(-s/\tau_2))/s ds \tag{A.10}$$

and

$$I_1 = \int_{t_1-t_0}^{t_1} \sigma^E(\lambda(t_1 - s))(\exp(-s/\tau_1) - \exp(-s/\tau_2))/s ds. \tag{A.11}$$

It is then clear that the three Equations (A.6), (A.7), and (A.9) form a nonlinear system which can be solved by the Newton–Raphson method for the three unknowns β, (αc), and τ_2. Convergence of $\beta^{(n)}$, $(\alpha c)^{(n)}$, and $\tau_2^{(n)}$ occur after a few iterations (the number depending on a given tolerance) and the parameter $c^{(n)}$ is obtained from the ratio $(\alpha c)^{(n)}/\alpha^{(1)}$. The above algorithm was coded and implemented on *Maple VI* [23], and we refer the reader to Drapaca [8] for the details. It is clear that the implementation of this algorithm requires loading data at fast strain rates. To our knowledge, the only work of this type was published long ago by Estes and McElhaney [12], and so that is what we used. As for the relaxation, we have used data obtained by the same laboratory but published separately [16], with the method discussed in Section 4.

References

1. ABAQUS/Standard. Version 6.2, Hibbit, Karlsson & Sorenson Inc. (2001)
2. Beatty, M.: Topics in finite elasticity: Hyperelasticity of rubber elastometers and biological tissues with examples. Appl. Mech. Rev. **40**, 1699–1734 (1987)
3. Biot, M.: General theory of three-dimensional consolidation. J. Appl. Phys. **12**, 155–164 (1941)
4. Carew, E., Talman, E., Boughner, D., Vesely, I.: Quasi-linear viscoelastic theory applied to internal shearing of porcine aortic valve leaflets. J. Biomech. Eng. **121**, 386–392 (1999)
5. Dortmans, L., Sauren, A., Rousseau, E.: Parameter estimation using the quasi-linear viscoelastic model proposed by Fung. J. Biomech. Eng. **106**, 198–203 (1984)
6. Drake, J., Kestle, J., Milner, R., Cinalli, G., Boop, F., Piatt, J.J., Haines, S., Schiff, J., Cochrane, D., Steinbok, P., MacNeil, N., collaborators: Randomized trial of cerebrospinal fluid shunt design in pediatric hydrocephalus. Neurosurgery **43**, 294–305 (1998)
7. Drake, J., Sainte-Rose, C.: The Shunt Book. Blackwell (1995)
8. Drapaca, C.: Brain biomechanics: Dynamical morphology and nonlinear viscoelastic models of hydrocephalus. PhD thesis, University of Waterloo, Canada (2002)
9. Drapaca, C., Sivaloganathan, S., Tenti, G., Drake, J.: Dynamical morphology of the brain's ventricular cavities in hydrocephalus. J. Theor. Med. **6**(3), 151–160 (2005)
10. Engin, A., Wang, H.: A mathematical model to determine viscoelastic behavior of *in vivo* primate brain. J. Biomech. **3**, 283–296 (1970)
11. Eringen, A.C.: Nonlinear Theory of Continuous Media, McGraw-Hill Series in Eng. Sciences, (1962)
12. Estes, M., McElhaney, J.: Response of brain tissue of compressive loading. ASME paper, 70-BHF-13 pp. 1–4 (1970)
13. Findley, W., Lai, J., Onaran, K.: Creep and relaxation of non-linear materials with an introduction to linear viscoelasticity. North-Holland Series in Applied Mathematics and Mechanics (1976)
14. Fung, Y.: Biomechanics: Mechanical Properties of Living Tissues, Springer, Berlin Heidelberg New York (1993)
15. Fung, Y., Perrone, N., Anliker, M.: Biomechanics: Its Foundations and Objectives. Englewood Cliffs, New Jersey, Prentince-Hall (1972)
16. Galford, J., McElhaney, J.: A viscoelastic study of scalp, brain, and dura. J. Biomech. **3**, 211–221 (1970)
17. Gurtin, M., Sternberg, E.: On the linear theory of viscoelasticity. Arch. Ration. Mech. Anal. **11**, 291–356 (1965)

18. Hakim, S., Venegas, J., Burton, J.: The physics of the cranial cavity, hydrocephalus and normal pressure hydrocephalus: Mechanical interpretation and mathematical model. Surg. Neurol. **5**, 187–210 (1976)
19. Huang, N., Lee, E.: Nonlinear viscoelasticity for short time ranges. Transactions of the ASME, J. Appl. Mech. **33E**, 313–321 (1966)
20. Kaczmarek, M., Subramaniam, R., Neff, S.: The biomechanics of hydrocephalus: Steady-state solutions for cylindrical geometry. Bull. Math. Biol. **59**(2), 295–323 (1997)
21. Kyriacou, S., Mohamed, A., Miller, K., Neff, S.: Brain mechanics for neurosurgery: Modeling issues. Biomechanics and Modelling in Mechanobiology **1:2**, 151–164 (2002)
22. Lee, J., Haberer, S., Pereira, C., Naimark, W., Courtman, D., Wilson, G.: High strain rate testing and structural analysis of pericardial bioprosthetic materials. In: Kambic H.E., Yokobori, A.T. (eds.) ASTM STP 11713, pp. 19–42. Philadelphia: ASTM (1994)
23. MAPLE, VI (n.d.), http://www.waterloomaple.com
24. Mendis, K., Stalnaker, R., Advani, S.: A constitutive relation for large deformation finite element modeling brain tissue. Transactions of the ASME, J. Biomech. Eng. **117**, 279–285 (1995)
25. Miller, K., Chinzei, K.: Constitutive modelling of brain tissue: Experiment and theory. J. Biomech. **30**(11/12), 1115–1121 (1997)
26. Miller, K., Chinzei, K.: Mechanical properties of brain tissue in tension. J. Biomech. **35**, 483–490 (2002)
27. Mooney, M.: A theory of large elastic deformation. J. Appl. Phys. **11**, 582–592 (1940)
28. Morland, L., Lee, E.: Stress analysis for linear visoelastic materials with temperature variation. Trans. Soc. Rheol. **IV**, 233–263 (1960)
29. Myres, B., McElhaney, J., Doherty, B.: The viscoelastic responses of the human cervical spine in torsion: Experimental limitations of quasi-linear theory, and a method of reducing these effects. J. Biomech. **24**(9), 811–817 (1991)
30. Nagashima, T., Tamaki, N., Matsumoto, S., Horwitz, B., Seguchi, Y.: Biomechanics of hydrocephalus: A new theoretical approach. Neurosurgery **21**(6), 898–904 (1987)
31. Nigul, I., Nigul, U.: On algorithms of evaluation of Fung's relaxation function parameters. J. Biomech. **20**(4), 343–352 (1987)
32. O'Hayon, B., Drake, J., Ossip, M., Tuli, S., Clarke, M.: Frontal and occipital horn ratio: A linear estimate of ventricular size for multiple imaging modalities in pediatric hydrocephalus. Pediatr. Neurosurg. **29**, 245–249 (1998)
33. Pamidi, M., Advani, S.: Nonlinear constitutive relations for human brain tissue. Transactions of the ASME **100**, 44–48 (1978)
34. Pena, A., Bolton, M., Whitehouse, H., Pickard, J.: Effects of brain ventricular shape on periventricular biomechanics: A finite-element analysis. Neurosurgery **45**(1), 107–116 (1999)
35. Rogers, T., Lee, E.: The cylinder problem in viscoelastic stress analysis. Q. Appl. Math. **22**, 117–131 (1964)
36. Rousseau, E., Sauren, A., van Hout, M., van Steenhoven, A.: Elastic and viscoelastic material behaviour of fresh and glutaraldehyde-treated porcine aortic valve tissue. J. Biomech. **16**(5), 339–348 (1983)
37. Sauren, A., Rousseau, E.: A concise sensitivity analysis of the quasi-linear viscoelastic model proposed by Fung. Transactions of the ASME, J. Biomech. Eng. **105**, 92–95 (1983)
38. Talman, E., Boughner, D.: In: Simon, B. (ed.) Shear Rate Affects Viscoelastic Measurements on Porcine Aortic Valve Tissue Tested in Shear, ASME Bioeng. Div. Publ. pp. 55–56 (1997)
39. Tenti, G., Drake, J., Sivaloganathan, S.: Brain biomechanics: Steady-state consolidation theory of hydrocephalus. Can. Appl. Math. Q. **7**(1), 93–110 (1999)
40. Ting, E.: Stress analysis for a non-linear viscoelastic compressible cylinder. Transactions of the ASME, J. Appl. Mech. **37E**, 1127–1133 (1970a)
41. Ting, E.: Stress analysis for a non-linear viscoelastic cylinder with ablating inner surface. Transactions of the ASME, J. Appl. Mech. **37**, 44–47 (1970b)
42. Ting, E.: Stress analysis for linear viscoelastic cylinders. AIAA J. **8**, 18–22 (1970c)
43. Tuli, S., O'Hayon, B., Drake, J., Clarke, M., Kestle, J.: Change in ventricular size and effect of ventricular catheter placement in pediatric patients with shunted hydrocephalus. Neurosurgery **45**(6), 1329–1335 (1999)
44. Tuli, S., O'Hayon, B., Drake, J., Kestle, J.: Change of ventricular size and effect of ventricular catheter placement of shunted hydrocephalus. Can. J. Neurol. Sci. **25**, S43 (1998) (Abstract)
45. Wineman, A.: Some results for generalized neo-hookean elastic materials. Int. J. Non-Linear Mech. **40**, 271–279 (2005)